

MULTITAPER SPECTRAL ESTIMATION: A GENERALIZED WINDOWS APPROACH

Nurgün Erdöl

Florida Atlantic University
Department of Electrical Engineering
Boca Raton, Florida 33431
USA

phone: + (1)561.297.3409, fax: + (1) 561.297.2336, email: erdol@fau.edu

ABSTRACT

A generalization of the multitaper spectral estimator is formulated and is shown to be equivalent to a generalized two-dimensional window, which allows a setting for non-stationary spectral estimation. The stationary case is specified as its restriction to a line in the two dimensional frequency plane. The formulation brings new tapers into consideration, and two of them are proposed and compared to the commonly used Slepian and sine-tapers.

1. INTRODUCTION

We generalize the multitaper spectral estimate [1][2] by defining the 2-dimensional estimate

$$\hat{S}(\omega_1, \omega_2) = \frac{1}{K} \sum_{k=0}^{K-1} X_k(\omega_1) X_k^*(\omega_2) \quad (1)$$

where

$$X_k(\omega_1) = \sum_{n=0}^{N-1} x[n] v_k[n] e^{-j\omega_1 n} \quad (2)$$

is the discrete-time Fourier transform (DTFT) of the data $x[n]$ of a zero mean random process x_n multiplied by the k^{th} window sequence $v_k[n]$. We will assume that the infinite extent data sequence $x[n]$ has DTFT $X(\omega)$. All DTFTs are 2π -periodic in ω and all frequency domain references, including integral limits, are over the principal domain.

The operation on the sequence can be written as the 2D periodic convolution integral (denoted by $**$)

$$\hat{S}(\omega_1, \omega_2) = X(\omega_1) X^*(\omega_2) ** \mathcal{A}_{K,N}(\omega_1, \omega_2) \quad (3)$$

where

$$\mathcal{A}_{K,N}(\omega_1, \omega_2) = \frac{1}{K} \sum_{k=0}^{K-1} V_k(\omega_1) V_k^*(\omega_2). \quad (4)$$

and $V_k(\omega)$ are the DTFTs of the tapers. For a narrow-band window function, the convolution of (3) is an estimate stabilizer. The IDFT of (3) yields the associated autocorrelation estimate

$$\hat{r}[n, m] = x[n] x^*[m] \alpha_{K,N}[n, m]. \quad (5)$$

where

$$\alpha_{K,N}[m, n] = \frac{1}{K} \sum_{k=0}^{K-1} v_k[m] v_k^*[-n]. \quad (6)$$

We call the transform pair of (4) and (6) the generalized window. The conventional multitaper spectral estimate (MTSE) $\hat{S}^s(\omega) = \hat{S}(\omega, \omega)$ is given by (1) and (3) for $\omega = \omega_1 = \omega_2$. Further, for separable windows, i.e., if $\mathcal{A}_{K,N}(\omega_1, \omega_2) = \beta(\omega_1) \beta^*(\omega_2)$, then we have the direct spectral estimate of the windowed Fourier transforms or the periodogram. The generalized windows version of MTSE [1] are, in general, not separable and hence cannot be reduced to a periodogram. The common tapers of MTSE are the Slepian [3] discrete prolate spheroidal sequences (DPSS) used by Thomson and minimum-bias and their approximate sine tapers proposed by Riedel and Sidorenko [4]. We reformulate the problem and show that the generalized form of (1) may be used to redefine the choice of tapers, to estimate both the spectrum and the autocorrelation and define measures for the goodness of each estimate.

2. STATIONARY PROCESS ESTIMATE

The expected values given in (3) and (5) are, respectively,

$$S(\omega_1, \omega_2) = S_x(\omega_1, \omega_2) * \mathcal{A}_{K,N}(\omega_1, \omega_2) \quad (7)$$

$$r[n, m] = r_x[n, m] \alpha_{K,N}[n, m] \quad (8)$$

where $S_x(\omega_1, \omega_2) = E[X(\omega_1)X^*(\omega_2)]$ is the true spectrum and $r_x[n, m] = E[x[n]x^*[m]]$ is the true autocorrelation. If the process is stationary,

$$S_x(\omega_1, \omega_2) = S_x^s(\omega_1) \delta(\omega_1 - \omega_2) \quad (9)$$

and the estimate mean (7) becomes

$$S(\omega_1, \omega_2) = \int_{\theta_1} S_x^s(\theta_1) \mathcal{A}_{K,N}(\omega_1 - \theta_1, \omega_2 - \theta_1) d\theta_1. \quad (10)$$

Restriction of $S(\omega_1, \omega_2)$ to the axis $\omega_1 = \omega_2$ yields the stationary multitaper estimate

$$S^s(\omega) = S(\omega, \omega) = S_x^s(\omega) * \mathcal{A}_{K,N}(\omega, \omega). \quad (11)$$

The IDFT of (11) is

$$r^s[n] = r_x^s[n] \alpha_{K,N}^s[n] \quad (12)$$

where

$$\alpha_{K,N}^s[n] = \frac{1}{K} \sum_{k=0}^{K-1} \sum_{m=0}^{N-1} v_k[m] v_k^*[m-n] \quad (13)$$

$$r_x^s[n] = r_x[n + m, m]$$

In the Thomson estimate, the number of windows is much less than the window length, i.e. $K \ll N$. When all the windows are used $K = N$, the window in (10) becomes

$$\mathcal{A}_{K,N}(\omega_1 - \theta, \omega_2 - \theta) = \frac{\sin((\omega_1 - \omega_2)N/2)}{\sin((\omega_1 - \omega_2)/2)} e^{-j\phi} \quad (14)$$

where $\phi = (\omega_1 - \omega_2)(N-1)/2$. Such invariance to shift by θ causes the spectral estimate to be a constant, proportional to the energy of the windowed signal and is given by $\hat{S}^s(\omega) = 2\pi \sum_{n=0}^{N-1} |x[n]|^2$. Similarly $S^s(\omega)$ be-

comes a constant proportional to the process variance. This result is also easily explained by noting the DPSS set $\{v_k[n]\}_{k=0}^{N-1}$ form a complete orthonormal basis in the space of N -length sequences and is thus norm preserving.

If the window is a 2D Dirac-delta impulse function at the origin of the 2D principal region, we have

$$\hat{S}^s(\omega) = |X(\omega)|^2 \quad (15)$$

and

$$S^s(\omega) = S_x^s(\omega). \quad (16)$$

3. UNBIASED ESTIMATES

Unbiased estimates of both the spectrum and the autocorrelation require that $\mathcal{A}_{K,N}(\omega) \rightarrow \delta(\omega)$ and $\alpha_{K,N}[n] \rightarrow 1$ for all n as $N \rightarrow \infty$. Since $\mathcal{A}_{K,N}(\omega) \leftrightarrow \alpha_{K,N}[n]$ are Fourier transform pairs, these limits are satisfied simultaneously. For finite N , how-

ever, $\alpha_{K,N}[n]$ can never be a rectangular window. Being an autocorrelation sequence, its z-plane zeros are in reciprocal symmetry around the unit circle. As the number of zeros increase with N , they will also move toward the unit circle. Its limit as $N \rightarrow \infty$ may be represented as the limit as $N \rightarrow \infty$ of a $(M \geq 2N - 1)$ -periodic sequence

$$\tilde{r}_N[n] = \begin{cases} 1 & -(N-1) \leq n \leq (N-1) \\ 0 & N \leq |n| \leq (M-N) \end{cases}. \quad (17)$$

Its discrete Fourier series expansion is

$$\tilde{r}_N[n] = \frac{R[0]}{M} + 2 \sum_{k=1}^{M-1} \frac{R[k]}{M} \cos\left(\frac{2\pi kn}{M}\right) \quad (18)$$

where $R[k]$ are the DFS coefficients of $\tilde{r}_N[n]$. The sine tapers of [4] can be extracted from this series by observing that $\cos(\frac{2\pi kn}{M})$ is the periodic autocorrelation of $\sin(\frac{2\pi kn}{M})$, and letting $M = 2(N+1)$. We may now formulate our objective as a linear combination of the following:

For a given N choose $\{w_k[n] \leftrightarrow W_k(\omega)\}_{k=0}^{K-1}$ so that

$$\mathcal{A}_{K,N}(\omega) = \frac{1}{K} \sum_{k=0}^{K-1} W_k(\omega) W_k^*(\omega) \approx \delta(\omega) \quad (19)$$

and

$$\alpha_{K,N}[n] = \frac{1}{K} \sum_{k=0}^{K-1} \sum_{m=0}^{N-1} w_k[m] w_k^*[m-n] \approx 1. \quad (20)$$

The choice of $K \leq N$ is for stabilizing the estimates. The equation pair above should be analyzed for the effect of the number of tapers, K and the rate of convergence to the desired values as N increases. Initially, however, it should help to discuss the structure of these quantities.

3.1 Choice of Tapers

The tapers used [1][4] have traditionally been derived from an orthonormal basis. We have shown in Section 2 that choice of $K = N$ results in the spectral estimate becoming a constant, true only for white noise. Completeness of the basis implies $\mathcal{A}_{N,N}(\omega) = 1$ and causes the spectral estimates being severely biased as $K \rightarrow N$. Given a taper, the lowest bias outside the main lobe is achieved when $K = 1$. Limiting $K \ll N$ brings the sum much closer to the desired result. Choice of Slepian sequences optimizes energy concentration [2] and tapers of [4] reduce bias, however it is not necessary that the tapers be derived from a basis. This flexibility allows the derivation of sequences with desired properties. Two examples follow.

Low order Slepian sequences of length N maximize an energy concentration in a frequency band $[-\beta, \beta]$ and are chosen based on a specified time-bandwidth product $P = N\beta$. Typical values for P are in the range 1.5 and 3.5. Smaller P cause the sequences to be ill defined. For a given P , bandwidth β gets smaller with increasing $2N$. A simple calculation shows that $2N$ length Slepian tapers truncated to length N (so that they can be tapers to length N signals) have much smaller main-lobe widths than either of the N length Slepian tapers or sine tapers. This advantage comes at the expense of significant increase in high frequency bias as seen in Figure 1.

Also shown in Figure 1 is a taper obtained by multiplying the sine tapers with the first Slepian sequence. The result is lower high frequency bias at the expense of slight widening of the main lobe.

3.2 Measures for Tapers

We use

$$\Pi(\mathbf{W}, K, N) = \int_{-\pi}^{\pi} \omega^2 \mathcal{A}_{K,N}(e^{j\omega}) d\omega \quad (21)$$

as a measure of concentration in the frequency domain and

$$\Theta(\mathbf{w}, K, N) = \frac{1}{2N-1} \sum_{n=-N+1}^{N-1} [1 - \alpha_{K,N}[n]]^2 \quad (22)$$

as a measure of flatness in the time domain. The parameters $\mathbf{W} = \{W_k(\omega)\}_{k=0}^{K-1}$ and $\mathbf{w} = \{w_k[n]\}_{k=0}^{K-1}$ are transform pairs.

Using the measures given by (21) and (22), we compared the Slepian sequences, sinusoidal tapers and $2N$ -length Slepian sequences truncated to length N and the Slepian-1-times-sine tapers. We have normalized the autocorrelation window so that

$$\alpha_{K,N}[0] = 1, \quad |\alpha_{K,N}[n]| \leq 1 \text{ for all other } n. \quad (23)$$

and equivalently

$$\frac{1}{2\pi} \int_{-\pi}^{\pi} \mathcal{A}_{K,N}(e^{j\omega}) d\omega = 1, \quad \mathcal{A}_{K,N}(e^{j\omega}) \geq 0. \quad (24)$$

4. TESTING AND RESULTS

We use the following notation for the tested windows:

1. \mathbf{W}_1 : Slepian sequences of length N .
2. \mathbf{W}_2 : Slepian sequences of length $2N$ truncated to length N .
3. \mathbf{W}_3 : Sine tapers
4. \mathbf{W}_4 : Slepian-1-times-sine tapers

All the sets above use the same number K of vectors. In sets 1 and 2 and 3, the complete set of N vectors form an orthonormal basis for N -length sequences.

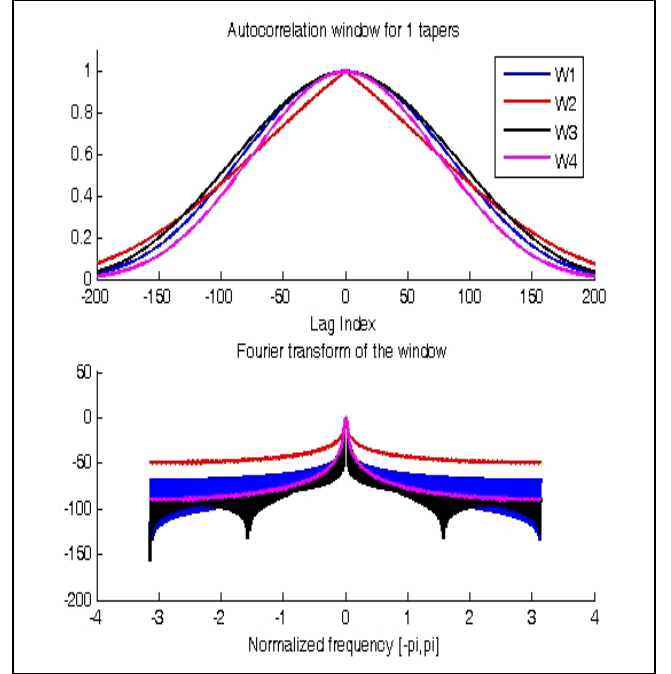


Figure 1. Autocorrelation (top) v lag and spectral magnitude (dB) v frequency ω of tapers W1 through W4. $N=256$, $K=1$.

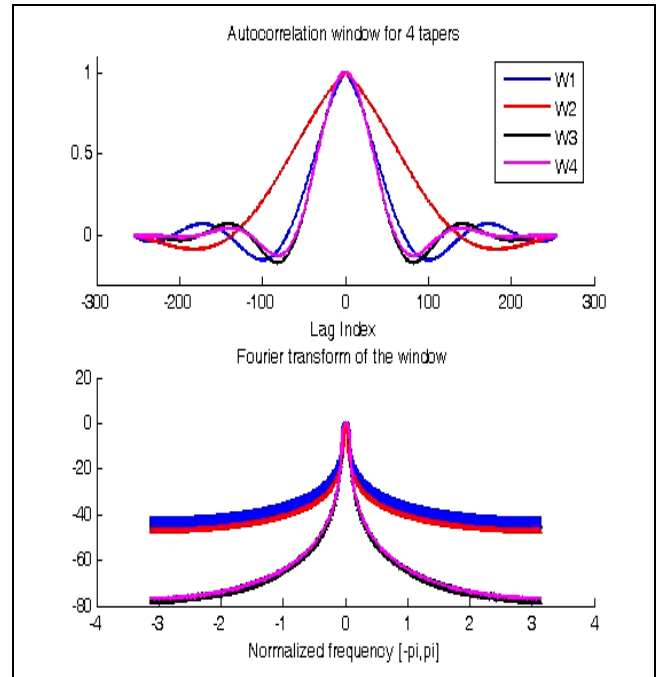


Figure 2. Same tapers as Figure 1 with $K=4$.

The two figures above demonstrate the effect of increased taper numbers and the performance of the different tapers. We note that the ordering of the tapers

based on high frequency bias changes with K because each taper has a different rate of change. A demonstration of this is shown in Figure 3.

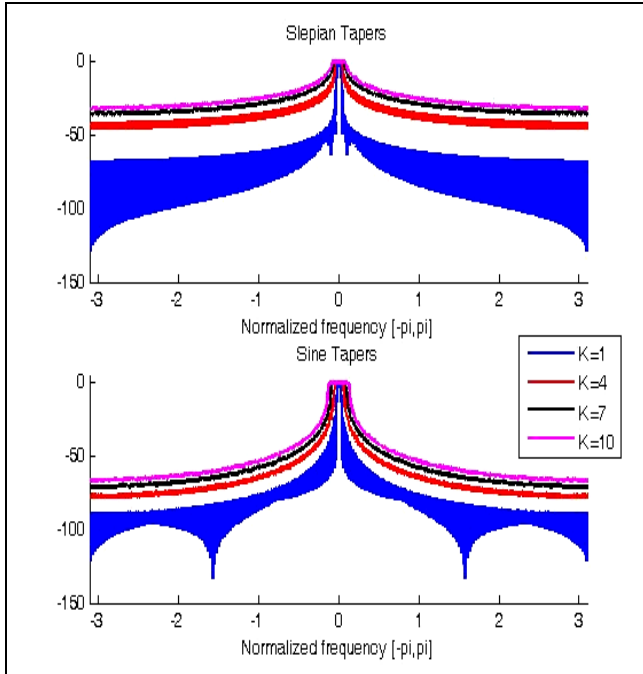


Figure 3. Spectra of the multitaper windows W_1 (top) and W_2 for $K=1,4,7,10$.

where $\text{sine}(W_1)$ and Slepian $2N$ W_2 window spectra have been plotted for odd values of K . We note that the former is uniformly increasing while the latter has its best value at $K=5$. Also note that the main-lobe width does not increase as fast in the latter as in the sine taper although clearly the high-frequency bias is much lower for sine tapers. These observations are quantified in for select values in the Tables 1 and 2.

5. CONCLUSION

We have offered a general formulation for multitaper spectral estimation that may be adopted for non-stationary spectral estimation, used to derive new tapers, may be weighted for use as an autocorrelation estimate and provides an alternate insight to the problem. We have offered two new tapers with different properties to lead the way.

6. ACKNOWLEDGEMENT

This material is based on work supported by National Institute of Aerospace under contract NAS1-02117-FAU10-04-6018FA.

Taper no.	W_1	W_2	W_3	W_4
1	0.0003	0.0127	0.0002	0.0003
2	0.0016	0.0071	0.0004	0.0006
3	0.0073	0.0093	0.0007	0.0009
4	0.0186	0.0135	0.0012	0.0013
5	0.0326	0.0207	0.0017	0.0018

Table 1. Computed frequency concentration error Π

Taper no.	W_1	W_2	W_3	W_4
1	0.0013	0.0044	0.0011	0.0027
2	0.0054	0.0024	0.0061	0.0124
3	0.0145	0.0043	0.0183	0.0280
4	0.0306	0.0079	0.0387	0.0515
5	0.0510	0.0146	0.0650	0.0804

Table 2. Computed autocorrelation error Θ .

REFERENCES

- [1] Thomson, D. J., Spectrum Estimation and Harmonic Analysis, Proceedings of the IEEE. Vol.70, No.9, pp. 1055-1096, September 1982.
- [2] Percival, D. B. and Walden, A. T., Spectral Analysis for Physical Applications. Cambridge University Press, 1993
- [3] Slepian, D., Prolate Spheroidal Wave Functions, Fourier Analysis, and Uncertainty-V: The Discrete Case, The Bell System Technical Journal, Vol. 57, No.5, pp.43-63, May-June 1978.
- [4] Riedel, K. S. and Sidorenko, A., Minimum Bias Multiple Taper Spectral Estimation, IEEE Tran. Sig. Proc., Vol.43, No.1, pp. 188-195, Jan. 1995
- [5] Hannsen, A. and Scharf, L., A Theory of Polyspectra for Nonstationary Stochastic Processes, IEEE Tran. Sig. Proc., Vol.51, No.5, pp. 1243-1252, May 2000